Contents lists available at http://qu.edu.iq

Al-Qadisiyah Journal for Engineering Sciences

Journal homepage: https://qjes.qu.edu.iq/

Experimental study of heat transfer using nanofluids in a coiled agitated vessel equipped with impeller propeller

Batool C. Shandal [a]*, ***H.I. Dawood*** [a], ***and Helen Onyeaka*** [b]

[a] *Department of Chemical Engineering College of Engineering, University of Al-Qadisiyah, Iraq*

[b] *School of Chemical Engineering, University of Birmingham, Birmingham, UK*

ARTICLE INFO

Article history:
Received 02 April 2023
Received in revised form 15 August 2023
Accepted 10 December 2023

Keywords:
Nanofluids
Methodology
MWCNT
Response Surface
Thermal conductivity

ABSTRACT

In this study, the heat transfer enhancement was made using multiwalled carbon nanotubes (MWCNTs) with distilled water (i.e . nanofluid) in a coiled agitated vessel. The thermal conductivity of the nanofluid at a volume fraction of (0.3 Vol%) was estimated with different parameters (temperature, propeller speed, flow rate, and time ultrasonication). The statistic program Minitab software 2019, using the Box–Behnken design (BBD) method, was used to identify the important and effective parameters of the process. The optimum parameters were found 55°C, 300 rpm, 1 L/min, and time ultrasonication of 100 min with enhanced thermal conductivity of about 76.5%.

1. Introduction

Heat transfer is an important part of how many devices and systems work. In a wide range of situations, the principles of heat transfer are used to raise, lower, or keep the temperature at the right level so that the desired process can happen at a controlled rate. Along with material transport and heat transfer, agitation is one of the most widely used operations in the chemical industry and is therefore an important chemical engineering operation. The process of combining or blending two substances is central to many branches of the chemical processing industry. In most cases, this is accomplished in a vessel fitted with an agitator. A machine like this is essential to any sector that deals with chemicals. Agitated vessels are commonly used to mix, aerate, and react to substances. Isothermal reactions, in which the temperature of the reactants and the reaction mixture are both constant, can be carried out in agitated vessels. To maintain a certain temperature in the reaction system, a helical coil or jacket may be used to provide an internal heat transfer surface. The jacket and the helical coil are sometimes used together to increase the heat transfer rate. Immersed helical coils are typically more advantageous to jackets for heat transfer because the heat transfer coefficient is greater in the coil than in the jacket, and the coil provides a sizable surface area in a small reactor volume. Although the effect of impeller position in the tank on heat transfer has been studied to some extent, much more research has been done on heat transfer coefficients in a coiled agitated vessel for different types of impellers. Most of the studies that have been published on the topic of heat transfer have been conducted by randomly fixing the flow rates of the cooling or heating medium and varying the agitator speed without adjusting the heat input. The heat transfer of some important industrial systems was recently investigated [1] [2], and more recently, a descriptive report on the impact of changing the heat input to the agitated medium on heat transfer efficiency in a coiled agitated vessel was presented [3] [4]. Experimental studies on heat transfer in coiled, agitated vessels have thus far only been conducted with Newtonian and non-Newtonian fluids (single- and two-phase liquids, solid-liquid suspensions, gas-solid suspensions, etc.). Suspending high-

* *Corresponding author.*
E-mail address *eng.chem.20.post.13 @qu.edu.iq* (*Batool C.Shandal*)

https://doi.org/10.30772/qjes.2023.145214.1062

thermal-conductivity solid particles in fluids is a novel technique to improve heat transfer performance. A long time ago, millimeter- or micrometer-sized particles were put into fluids to help heat move through them more quickly. However, there are significant drawbacks associated with such suspensions, including settling, blocking flow channels [5] [6], [7] [8] erosion of heat transfer devices, and a higher pressure drop. This is why there has been so much focus on improving heat transfer via different methods as of late. Many people are interested in using energy-efficient heat transfer fluids because of the increased heat transfer capabilities they provide. These fluids are formed by suspending nano-sized particles in conventional heat transfer fluids. Choi and Eastman came up with the name "nanofluid" to describe this new category of nanotechnology-based heat transfer fluids (liquid suspensions containing particles; [9][10]with dimensions much smaller than 100 nm. Nanofluid's benefits include:(1) greater thermal conductivities than those suggested by standard macroscopic models, (2) excellent stability (3) Suspension of particles less than a millimeter or a micrometer in size incurs no cost from an increase in pressure drop or pipe wall erosion. This study predicts that nanofluids could be used as a agitated medium in a coiled agitated vessel. This is because nanofluids have become very popular as a way to transfer heat. Research work on heat transfer using nanofluids has only been conducted in a few different types of heat exchangers, including: (1) circular tubes (horizontal/vertical, heated/unheated) [11] [12] , [13] [14], (2) shell and tube, (3) double pipe, (4) multi-channel heat exchangers; and (5) rectangular microchannels. All of these studies concluded that incorporating nanoparticles into a base fluid improved convective heat transfer over the base fluid alone, with the degree of improvement increasing with nanoparticle concentration. Most heat transfer investigations employing nanofluids are limited to heat exchangers. The literature suggests utilizing nanofluids as heat transfer fluids in agitated vessels, which has not been noted. This research presents the heat transfer properties of MWCNTs/water nanofluid in a propeller-agitated tank.

2. Development of MWCNTs/water nanofluids

This work produced nanofluids using MWCNTs from the Tsinghua Nafine Nanoparticle Commercialization Engineering Centre (China). They were pressure-catalyzed from hydrocarbons on a nanocatalyst. An SEM image of Fig. 1 shows the MWCNTs particle shapes and sizes at 135k× magnification. Notably, the size of MWCNTs particles ranged from 26.64 nm to 28.55 nm. The BET method was used to measure the material pore size, volume distribution, and specific surface area in nitrogen adsorption and desorption environments. However, BET mechanics were carried out using this method, beginning with sample preparation. The samples usually have moisture and could have other contaminants that must be removed. The removal can be done by evacuating or purging the sample with heated inert gas. In order to desorb the moisture and other impurities that would otherwise affect the analysis. After preparation, the sample is evacuated and then cooled to cryogenic temperatures of about – 196 ℃ liquid nitrogen temperature. The actual measurement of gas sorption begins by exposing the sample to a low pressure of adsorptive gas. As the gas pressure rises, the amount of adsorbed at the surface rises until a monolayer is formed.

Additionally, as the adsorption process continuously moves through multilayer formation, the molecules are adsorbed. The beginning of mesoporous filling as the gas pressure further increased. The smaller pores fill before the larger pores; if the pores are not large, they can be filled completely. Thus, it completes the adsorption at the isotherm (Mohan et al., 2020). The results of BET surface area analysis were BET Surface Area: 251.5623 ± 2.0756 m²/g, which is a desirable quality in heat transfer applications. The pore volume and average particle size were found to be 0.612099 cm³/g and 23.8510 nm, respectively. These are the properties of a mesoporous substance.

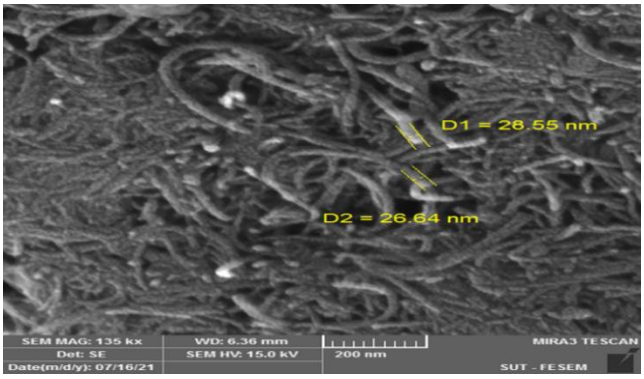

Figure 1. SEM micrograph of MWCNTs

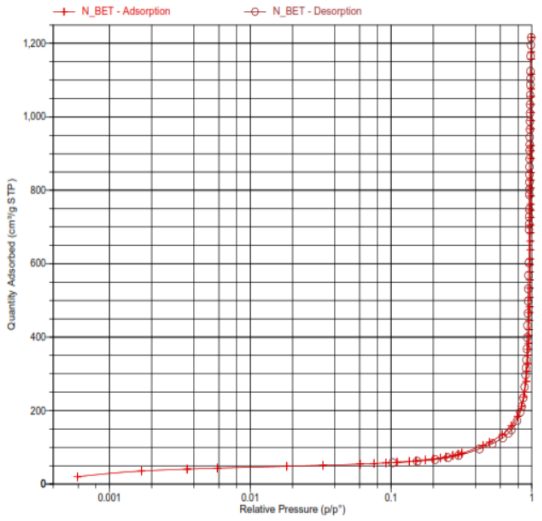

Figure 2. BET N2 adsorption-desorption isotherm of multiwalled carbon nanotubes Results of experimental design

The adsorption-desorption plot for MWCNTs was presented in Fig.2. Nitrogen uptakes rose as the relative pressure increased in the pressure range. MWCNTs exhibited type I features with a hysteresis loop at 0.1≤ p/p≤1, which is consistent with the categorization of the International Union).

XRD analysis is an effective and non-destructive technique used to analyze crystalline materials. It provides information about the crystal structures, phases, and preferred orientation of crystals. This test is also concerned with the rest of the composition parameters of materials, such as nanometer materials crystal size, crystal structure, sample phase, and the purity of the ordinary and nanometer materials [15]. The diffraction peaks of X-rays result from the constructive interference of a single-wavelength X-ray beam scattered at specific angles from a set of crystalline planes of the material. The XRD results were obtained for the product MWCNTs. There are only two peak point values achieved by XRD for MWCNTs, which are25.65 ˚θ and 44.2˚θ shown in Fig .3. The XRD result also gives information about the lattice that it is primitive and crystalline in nature. It has the same reference as the standard MWCNTs structure [16][17].

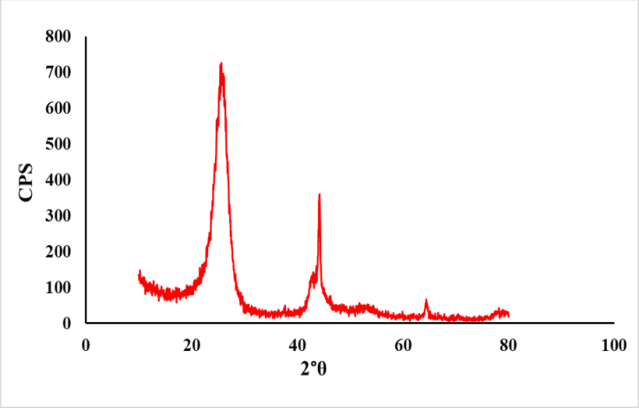

Figure 3. The Pattern of the XRD regarding porous MWCNTs

3. Experimental setup

The MWCNTs - are prepared in distilled water using sonication of the nanofluids. MWCNTs and water were mixed in a sonicated for a periodic of time using a water bath sonicator. MWCNTs at constant 0.3 Vol%.

Table 1. Process parameters and their levels for heat transfer in agitated vessel

Variable	Range
Temperature	(55 -77 °C)
Speed	(125 -300 r/min)
Flow rates	(1- 2 Litter/min)
Time ultrasonication	(40- 100 min)

The agitated vessel system was composed of a cylindrical capacity (15 L) made of metallic (aluminum and platinum) of 30 cm inner diameter and 32 cm height with an ellipsoidal lid used as a test vessel. An impeller shaft of 0.01 m diameter and the cooling water inlet and outlet. Agitation was carried out by a propeller agitator with a diameter of 10 cm (1/3 of tank diameter) and 3 blades. Propeller agitator speed was varied from 120 to 540 r/min) by means of variable speed electrical type motor. Swirling and vortex formation inside the liquid pool could be prevented by using four wall baffles, each of them having width of 2.5cm (1/12 of tank diameter) and height of 29.5 cm. These baffles were welded to the inside wall of the test vessel by dividing the periphery into four equal segments. The temperature inside the bowl is controlled by the control system. A helical coil of 8 turns was fabricated out of copper tube of 11.5 mm inner diameter, 13mm outer diameter and 4.71 m length. Average outside coil diameter was 20 cm with 2.8 cm spacing between two consecutive coil turns. The helical coil was submerged in the pool of liquid medium being agitated up to a height of 22.5 cm (3/4 of tank diameter) and water as cooling medium was circulated through the helical coil with the help of centrifugal pump and the flow rate was measured by means of a calibrated rotameter.Fig.4 shows a schematic diagram of the dimension of the agitated vessel . Fig.5 shows a schematic diagram of the dimension of the helical coil.

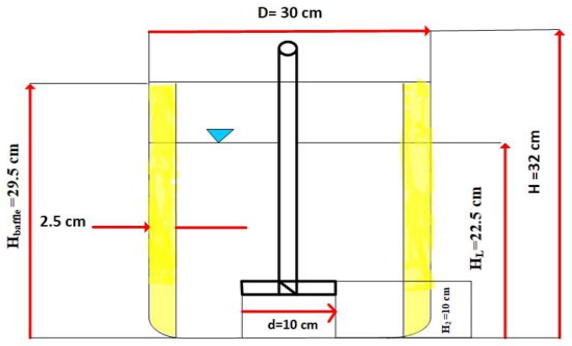

Figure 4. Diagram showing the dimensions of the agitated vessel.

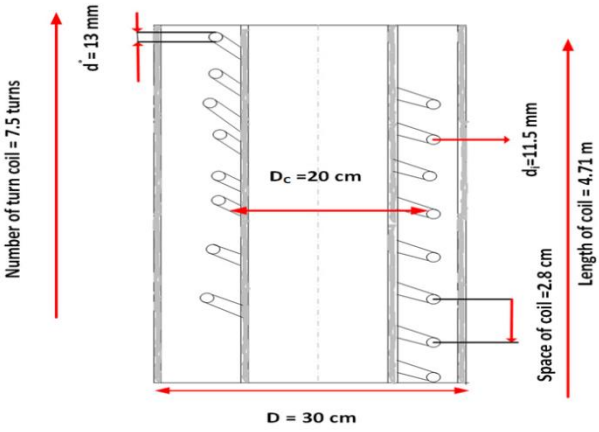

Figure 5. Schematic diagram of helical coil design.

Fig.6 depicts the experimental setup's schematic design. The interior temperature of a cylindrical container with an inner diameter of 0.3 m and a height of 0.32 m was monitored using a circular cover with a hole at the top in which a sensor could be installed. It has pipelines to cool the incoming and outgoing water, as well as a three-blade fan with a diameter of 10 cm (1/3) of the tank's diameter.

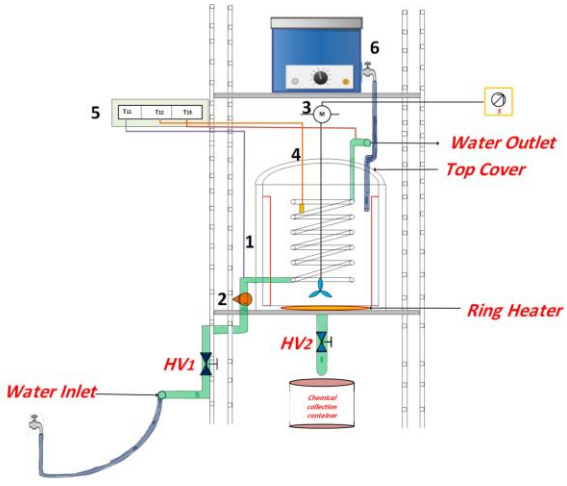

Figure 6. Experimental setup

The propeller agitator speed can range from 120 to 540 r/min when powered by a variable-speed electrical motor. Temperatures throughout the experiment ranged from 30 °C to 90 °C, and the heat input was changed from 400 to 2200 watts. Four baffles, each with a width of 0.025 m (1/12 of the tank diameter) and a height of 0.32 m, may be used to stop swirling and vortex development within the liquid pool. By cutting the edge into four equal pieces, these baffles were welded to the test vessel's interior wall. The copper tube with an inner diameter of 0.0115 m, an outside diameter of 0.013 m, and a length of 4.57 m was used to create a 7.5-turn helical coil. The distance between two successive coil turns was 0.028 m, with an average outer coil diameter of 0.2 m. A centrifugal pump circulated water through the helical coil as the cooling medium, and a calibrated rotameter was used to monitor the flow rate. The helical coil was immersed in a pool of liquid medium that was being stirred up to a height of 0.3 m (3/4 of the tank's diameter). The temperatures of the agitated liquid medium at the top and bottom locations, as well as the temperatures of the cooling water at the input and outflow, were recorded using a single digital temperature indicator.

4 . Experimental procedure

In the beginning, distilled water was used for the tests, and afterward, a constant (0.3 vol%) concentration of MWCNTs in water nanofluid was used. Throughout the experiment, the procedure's follow-in sequences were maintained. (1) Nanofluids in a 15-liter container were added to the agitated tank. (2) The heaters' power input was predetermined, and the stabilizer was turned on. (3) The agitator's speed was changed by using an electrical motor with a variable speed set at a certain value. (4) The experiment was left to continue until a steady state was reached. The flow rate of cooling water via helical cooling was varied (between 1-2 liters per minute) to remove the heat provided by heaters from the liquid being agitated. (5) The liquid temperature of the vessel at its top and bottom, as well as the intake and outlet temperatures of the cooling water, were measured at a steady state. (6) At a given heat input, the agitator's speed was varied, and data were collected once it reached a steady state. (7) The heater's heat input and the agitator's rotating speed were both changed, and readings were collected for each input.

5. Models for the calculation.

5.1 Nanofluid properties

Nanofluid's thermophysical characteristics The following formulas are used to compute the thermophysical parameters of the MWCNTs/water nanofluid, including density, viscosity, specific heat, and thermal conductivity. According to the [18], the density equation of the nanofluid is determined and is given as

$$\rho_{nf} = \varphi\,\rho_p + (1-\varphi)\rho_{bf} \quad (1)$$

Where; ρ_{nf} , ρ_p and ρ_{bf} are the densities of nanofluid, particles, and base fluid in (kg/m^3), respectively, while φ is the nanofluid volume fraction.
The existing relations can calculate the nanofluid viscosity for a two-phase mixture. The well–known Einstein formula [19] [20] was utilized by Drew and Passman [21] [22] for evaluating the effective viscosity of a linearly viscous fluid that contains a suspension of tiny solid particles;

$$\mu_{nf} = (1+2.5\,\varphi)\,\mu_{bf} \quad (2)$$

Where; μ_{nf} and μ_{bf} are the viscosities of the nanofluid and base fluid in (kg/m· s), respectively. For low-volume concentrations, less than 5% can be used.
The use of Xuan and Roetzel's [23][24] equation the nanofluid-specific heat was estimated as follows:

$$(\rho C_p)_{nf} = \varphi(\rho C_p)_p + (1-\varphi)(\rho C_p)_{bf} \quad (3)$$

Where; $\mathbf{C_{p_{nf}}}$, $\mathbf{C_{p_p}}$, and $\mathbf{C_{p_{bf}}}$ are the specific heats in (J/ kg. K) of nanofluid, particles and base fluid respectively.

5.2 Heat Transfer Coefficient Models

The system's geometry, the agitated liquid's characteristics, and the mixing intensity, which is determined by the agitator's design and rotational speed, all influence the heat transfer rate between the cooling water cycling within the helical coil and the agitating fluid.

In this investigation, convection heat transfer is used to move heat from the heated fluid in the agitated vessel to the cooler water flowing in the helical coil.The thermophysical properties of cooling water were evaluated at average temperature measured by temperature indicators T_{in} and T_{out} whereas the thermo physical properties of agitated fluid were evaluated at average temperature bath temperature measured by temperature indicators T_B .
calculate the mean film temperature T_f at which the properties of the water inside the cooling tube are determined by the following equation;

$$T_f = \frac{T_{wall} + \left(\frac{T_{in}+T_{out}}{2}\right)}{2} \quad (4)$$

Where; T_{wall} is the wall temperature of the cooling coil in (K), T_i and T_{out} inside and outside cooling water in (K).

At the mean film temperature calculated fluid properties are $\rho_{cooling\ water}$ $Cp_{cooling\ water}$, $K_{cooling\ water}$, $Pr_{cooling\ water}$, $\mu_{cooling\ water}$
Where; $\rho_{cooling\ water}$ the density of cooling water in (kg/m^3), $C_{p\ cooling\ water}$ is the specific heat capacity of cooling water at a given temperature in (J/ kg. K), $K_{cooling\ water}$ is the thermal conductivity of cooling water in (W/m· K), $Pr_{cooling\ water}$ is Prandtl number (dimensionless) and $\mu_{cooling\ water}$ the viscosities of cooling water at a given temperature in (kg/m· s).
Evaluate the Reynolds number to determine if the flow is laminar or turbulent.

$$Re = \frac{\rho_{cooling\ water}\ u\ d_i}{\mu_{cooling\ water}} \qquad Cp_{cooling\ water} \quad (5)$$

Where; u velocity of the coil (m/s) and d_i is the inside diameter of the coiled tube in (m).
Calculation of heat transfer in turbulent flow, $2500 < Re < 1.25 * 10^5$ and $0.6 < Pr_{cooling\ water} < 100$ is recommended by [13] [21].

$$Nu = 0.023\ Re^{0.8}\ Pr^{n} \quad (6)$$

Where; Nu is the Nusselt number for the inside heat transfer coefficient (dimensionless). The properties in this equation are evaluated at the average mean film temperature, and the exponent has the following value:
n= 0.4 for heating of the fluid
Calculate the heat-transfer coefficient inside cooling water hi (W/m^2. K).

$$Nu = \frac{h_i\, d_i}{K_{cooling\ water}} \quad (7)$$

As the test vessel was completely insulated to prevent heat losses during agitation, the actual rate Q of heat transfer was taken is given as:

$$Q = Q_{1_{supplied}} = Q_{2_{gained}} \quad (8)$$

Where; Q_1 and Q_2 are the heat supplied by the heater to the agitated medium and the heat gained by the cooling medium in (W), respectively, and given by:

$$Q = Q_{2_{gained}} = m\, C_{p\ cooling\ water}\ (T_{out} - T_{in}) \quad (9)$$

Where m is the mass flow rate of water in (kg/s).

By using the equation below, the overall heat transfer coefficient is calculated [14] [25].

$$U_\circ = \frac{Q}{A_\circ\,(T_{wall} - \frac{(T_{in} - T_{out})}{2})} \quad (10)$$

Where; $U_\circ$ in is the overall heat transfer coefficient (W/$m^2.K$), $A_\circ$ is the outside surface area of the helical coil in (m^2).
Where $A_\circ$ is given by

$$A_\circ = \pi\, d^\circ L \quad (11)$$

Where; $d^\circ$the outside diameter of the coiled tube in (m) and is the length of the helical coil in (m).

Knowing $U_\circ$ and h_i , the outside heat transfer coefficient is calculated using the relation [15] [10].

$$h^\circ = \frac{1}{\left\{\frac{1}{U_\circ} - \left[\frac{1}{h_i}\ \frac{d^\circ}{d_i} + \left(\frac{X_w}{k_c}\right)\left(\frac{d^\circ}{d^\circ - d_i}\right) ln\frac{d^\circ}{d_i}\right]\right\}} \quad (12)$$

Where; h° is the outside heat transfer coefficients in (W/$m^2.K$) d_i is the inside diameter of the coiled tube in (m) respectively, X_w is the helical coil wall thickness in (m) and k_c is the thermal conductivity of coil material in (W/m· K) .
calculate the thermal conductivity of nanofluids $K_{nanofluids}$ in (W/m.k) by equating equations (13) and (14).

$$\text{Nu} = \frac{h^\circ d^\circ}{K_{nanofluids}} \quad (13)$$

$$\text{Nu} = 0.64 Re^{0.67} Pr^{0.33} \left(\frac{\mu}{\mu_{wall}}\right)^{0.14} \quad (14)$$

The conditions for using equation (14) [16][26] must be propeller, 3 blades, transfer to vessel wall, Re > 5000:

Where; *Re* Reynolds number For agitator (dimensionless)

$$Re = \frac{\rho\, N\, {D_a}^2}{\mu} \quad (15)$$

ρ density of nanofluids, N rotating speed of agitator (revolution per second) (rps), D_a diameter of the Agitator (m), μ and μ_{wall} are the viscosities of nanofluids at a given temperature and wall temperature in (kg/m· s) respectively.
And then calculate the Thermal conductivity enhancement **(**%) (dimensionless) of nanofluids [17] [16] in optimum conditions using the relation :

$$\textit{Thermal conductivity enhancement (\%)} = \frac{k_{nf} - k_{bf}}{k_{bf}} * 100 \quad (16)$$

Where k_{nf} and k_{bf} are, respectively, the thermal conductivity of the nanofluid and base fluid in (W/m.K).

6. Results and discussions

6.1 Design of experiments

Response surface methodology (RSM) is summarized as a collection of mathematical and statistical tools for determining a regression model equation that correlates an objective function with its independent variables [18] [2]. BBD was adopted to examine the impact of process variables on the thermal conductivity of nanofluids. The thermal conductivity of nanofluids (Knanofluid /m. K) was taken into account as a response. Table 1 shows the temperature (°C) (X1), speed (r/min) (X2), Flow rates(L/min) (X3) and time ultrasonication(min)(X4) were taken as process parameters, while Table 2 shows the scales of the process components were designated as follows: low (-1), middle or center point (0), and high level (1). Table 1 shows the process parameters with their selected levels while Table 3 shows the experiments array provided by BBD for the current work, which was obtained by the Minitab-19 program.

Table 2. Process variables with their level for heat transfer for the agitated vessel.

Process parameters	Level Box–Behnken		
Levels that are coded	Low(-1)	Middle (0)	High (+1)
X1- Temperature (°C)	55	66	77
X2- Speed (r/min)	125	213	300
X3-Flow rates(L/min)	1	1.5	2
X4-time ultrasonication (min)	40	70	100

In this work, the following second-order model with the least-squares approach was used to determine the correlation between the thermal conductivity of nanofluids and its independent variables.

$$Y = \beta_0 + \sum \beta_i x_i + \sum \beta_{ii} x_i^2 + \sum \beta_{ij} x_i x_j \quad (17)$$

Where knano fluid (W/m.k)is termed as Y, i and j refer to patterns index numbers, $\beta_{.0}$ is intercept term, x_1, x_2 … x_k are coded form of process variables. $\beta_{.i}$ refers the main effect of first-order(linear), $\beta_{.ii}$ represents the main effect of second-order and the interaction effect is denoted by $\beta_{i.j}$.

Table 3. Box- Behnken experimental design

Run	Bulk	Coded levels				Real value			
		x_1	x_2	x_3	x_4	Temperature (°C), X1	Speed (r/min) , X2	Flow rates(L/min),X3	time ultra (min), X4
1	1	1-	1-	0	0	55	125.0	1.5	70
2	1	1	1-	0	0	77	125.0	1.5	70
3	1	1-	1	0	0	55	300.0	1.5	70
4	1	1	1	0	0	77	300.0	1.5	70
5	1	0	0	1-	1-	66	213	1.0	40
6	1	0	0	1	1-	66	213	2.0	40
7	1	0	0	1-	1	66	213	1.0	100
8	1	0	0	1	1	66	213	2.0	100
9	1	1-	0	0	1-	55	213	1.5	40
10	1	1	0	0	1-	77	213	1.5	40
11	1	1-	0	0	1	55	213	1.5	100
12	1	1	0	0	1	77	213	1.5	100
13	1	0	1-	1-	0	66	125.0	1.0	70
14	1	0	1	1-	0	66	300.0	1.0	70
15	1	0	1-	1	0	66	125.0	2.0	70
16	1	0	1	1	0	66	300.0	2.0	70
17	1	1-	0	1-	0	55	213	1.0	70
18	1	1	0	1-	0	77	213	1.0	70
19	1	1-	0	1	0	55	213	2.0	70
20	1	1	0	1	0	77	213	2.0	70
21	1	0	1-	0	1-	66	125.0	1.5	40
22	1	0	1	0	1-	66	300.0	1.5	40
23	1	0	1-	0	1	66	125.0	1.5	100
24	1	0	1	0	1	66	300.0	1.5	100
25	1	0	0	0	0	66	213	1.5	70
26	1	0	0	0	0	66	213	1.5	70
27	1	0	0	0	0	66	213	1.5	70

Analysis of variance (ANOVA) was achieved, and after that, the regression coefficient (R2) was computed to determine the model's fit shows the process parameters with their selected levels.

6.2 Results of experimental design

According to BBD design, 27 runs were performed to investigate the optimum conditions for the thermal conductivity of nanofluids. Table 4 summarizes experimental findings regarding the thermal conductivity of nanofluids ($K_{nano\ fluids}$ W/m. K).

The table summarizes the experimental results for the thermal conductivity of MWCNTs. Table 5 shows that the thermal conductivity of nanofluids was in the range

of (12.5200-49.3683) W/m. K). As a preliminary inspection, a comparison between run (1) and run (2) showed that the temperature has a considerable impact on the thermal conductivity of nanofluids, where $k_{nanofluids}$ from 12.8677W/m. K to 12.5200W/m. K making a difference of 0.3477 as temperature increased from 55 to 77°Cat flow rate 1.5 Litter/min, speed 125 r/min and time ultrasonication 70 min When the comparison between run (21) and (22) showed that speed in its effects on the thermal conductivity of nanofluids where $k_{nanofluids}$ increasing from 12.7300 to 30.4866W/m. K) making a difference of 17.7566W/m. K, while the flow rate in runs 18 and 20 increases from 1 to 2 L/min, the thermal conductivity decreases from 34.3572 to 15.0434 W/m.K makes the difference 19.3138. As seen in Table 5, when the time ultrasonication increased from 40 to 100 min, the thermal conductivity increased from 12.7300 to 12.8572 W/m.K in different of 0.1272 W/m.K However, the precise effect of these parameters can be observed via ANOVA results. Using Minitab-19 software, results of the thermal conductivity of nanofluids were analyzed, and a quadratic model for the effectiveness of $k_{nanofluids}$ elimination expressed in terms of real process parameters was formulated as follows:

$$k_{nanofluids} = 34.1\text{-}0.034X1\text{+}0.2558\ X2\text{-}44.95X3\ \text{-}0.0099\ X4\text{-}0.00025X1*X1\ \text{+}0.00003\ X2*X2\ \text{+}14.42X3*X3\text{+}0.000069\ X4*X4\ \text{-}0.000165\ X1*X2\ \text{+}0.0332\ X1*X3\text{+}0.00022X1*X4\text{-}0.09262\ X2*X3\text{-}0.000006\ X2*X4\text{-}0.0072\ X3*X4 \quad (18)$$

WhereKnanofluid is the response, and X.1, X.2, X.3, and X4 are temperature, speed, flowrate, and time ultrasonication, respectively. At the same time, the interaction effect of all model parameters is represented by X.1X.2, X.1X.3, and X.2X.3. The main effects of parameters such as temperature, speed, flow rate, and ultrasonication time are depicted for X.1, X.2, X.3 and X4, respectively. The expected values were computed and summarized in Table 6 using equation 18. In eq. 18, the positive coefficient in front of any parameter reveals that the thermal conductivity increases with its increase and vice versa. The acceptability of BBD was identified through the use of analysis of variance (ANOVA). It is an analytical technique that utilizes Fisher's F- and P-tests to determine the model's and its parameters' significance [19] [13]. Generally, bigger F-values and smaller p-values indicate that the coefficient terms are more important [20][24]. The response surface model is also illustrated in Table 6. This table contains DF, which represents the degree of freedom of the model and its parameters, and the statistical terms are represented by the sum of the square (Seq. SS), the adjusted sum of the square (Adj. SS), and the adjusted mean of the square (ADJ. MS), respectively. P-values of (0.0001>) and an F-value of (169.15) were obtained, which elucidate that the regression model is highly significant. The model's coefficient of multiple correlations was 0.995.

The adjusted multiple correlation coefficient (ADJ. R2) equals 0.9945, while the predictable multiple correlation coefficient (pred. R2) equals to 0.9854. This model was well-matched since the difference between them was less than 0.00091 [21] [1] . In the present study, the lack-of-fit P-value (0.741 > 0.05) indicates that the lack of model fit was not statistically significant in comparison to the pure error.

Table 5. Experimental results of Box–Behnken design for thermal conductivity of nanofluids

Run	Bulk	Parameter $K_{nanofluid}$ (W/m.K)					
		Temp (°C)	Speed r/min	Flow rates L/min	time ultrasonication min	Actual	Predicted
1	1	55	125.0	1.5	70	12.8677	12.4300
2	1	77	125.0	1.5	70	12.5200	11.9450
3	1	55	300.0	1.5	70	30.9079	31.4692
4	1	77	300.0	1.5	70	29.9234	30.3473
5	1	66	213	1.0	40	34.9096	34.8854
6	1	66	213	2.0	40	15.3461	15.4141
7	1	66	213	1.0	100	35.3203	35.2385
8	1	66	213	2.0	100	15.3270	15.3374
9	1	55	213	1.5	40	22.0014	21.9899
10	1	77	213	1.5	40	20.9985	21.0415
11	1	55	213	1.5	100	21.9791	21.9832
12	1	77	213	1.5	100	21.2661	21.3247
13	1	66	125.0	1.0	70	20.5490	21.6123
14	1	66	300.0	1.0	70	49.3683	48.4376
15	1	66	125.0	2.0	70	9.0528	10.0306
16	1	66	300.0	2.0	70	21.6631	20.6469
17	1	55	213	1.0	70	35.6093	35.5545
18	1	77	213	1.0	70	34.3572	34.3854
19	1	55	213	2.0	70	15.5642	15.5027
20	1	77	213	2.0	70	15.0434	15.0649
21	1	66	125.0	1.5	40	12.7300	12.1948
22	1	66	300.0	1.5	40	30.4866	30.9465
23	1	66	125.0	1.5	100	12.8572	12.3640
24	1	66	300.0	1.5	100	30.5520	31.0539
25	1	66	213	1.5	70	21.5483	21.5526
26	1	66	213	1.5	70	21.5456	21.5526
27	1	66	213	1.5	70	21.5638	21.5526

6.3 The Influence of process factors on the thermal conductivity of MWCNTs.

The interaction impacts of the chosen factors on the answer may be graphically shown using RSM. The effect of temperatures on the velocities is seen in Fig. (7-a, b). Fig. 7(a) shows a response surface plot, and Fig. 7(b) depicts a contour plot. A contour plot's shape may provide important information about the nature and scope of an interaction. The surface pattern revealed an increase in velocity from 150 to 300 revolutions per minute (r/min) across the board, regardless of temperature. It serves as a standard against which results from nanofluid studies may be evaluated. A helical cooling coil is immersed in the pool of agitated liquid, drawing heat from the bulk liquid and transferring it to the water passing through the coil. Agitation makes high temperature distribution throughout the vessel possible, which also boosts the overall transfer efficiency. Nanoparticles suspended in a base fluid provide a large surface area, facilitating greater heat transfer.

A large number of atoms on the surfaces of small particles (20 nm or less) are available for quick thermal interaction [22] [20]. The fact that the particles can move around is also a benefit because it could lead to fluid convection, which speeds up heat transfer. The experimental results of the effect of propeller speed on heat transfer for water and MWCNTs/water nano-fluid at constant volume fractions of 0.3% using a propeller agitator are presented in Fig. 7. This Figure shows that as the agitation speed rises, so does the heat conductivity. This is because the higher the propeller agitator's speed, the more turbulence is created in the medium, and therefore, heat is transferred more efficiently. It is also observed that when heat is added, the temperature of the bath rises. The heat transfer force is increased with a larger temperature gap between the bath and the object being heated. Because of this effect increases the heat transfer coefficient [23] [12].

Fig.8 (a,b) shows the influence of temperature on the thermal conductivity for different values of flow rates 1-2 L/min and temperature. Fig. 8-a shows that the thermal conductivity decreases significantly with increasing flow rate. An increase in the outside temperature can indeed be achieved, especially with a decrease in the flow rate in the heating systems. According to different researchers, the outlet temperature is a function of the coolant flow rate [24] [6]. Fig.9 (a, b) depicates the relationship between the nanofluid temperature and preparation time ultrasonic, as well as their effect on the nanofluid thermal conductivity.

Table 6. Analysis of variance for thermal conductivity of mwcnts

SOURCE.	DF	ADJ SS	ADJ MS	F-VALUE	P-VALUE
MODEL.	14	2368.11	169.15	337.09	0.000>1
LINEAR	4	2216.04	554.01	1104.06	0.000>1
X1	1	1.94	1.94	3.86	0.073
X2	1	1051.40	1051.40	2095.29	0.000>1
X3	1	1162.64	1162.64	2316.97	0.000>1
X4	1	0.06	0.06	0.11	0.741
SQUARE	4	86.09	21.52	42.89	0.000>1
$X1^2$	1	0.00	0.00	0.01	0.924
$X2^2$	1	0.00	0.00	0.01	0.936
$X3^2$	1	69.28	69.28	138.06	0.000>1
$X4^2$	1	0.02	0.02	0.04	0.843
2-WAY INTER	6	65.99	11.00	21.92	0.000>1
X1*.X2	1	0.10	0.10	0.20	0.661
X1*.X3	1	0.13	0.13	0.27	0.615
X1*.X4	1	0.02	0.02	0.04	0.841
X2*.X3	1	65.68	65.68	130.90	0.000>1
X2*.X4	1	0.00	0.00	0.00	0.966
X3*.X4	1	0.05	0.05	0.09	0.767
ERROR	12	6.02	0.50		
LACK OF FIT	10	6.02	0.60	6250.72	0.000>1
PURE-ERROR	2	0.00	0.00	337.09	0.000>1
TOTAL	26	2374.13	169.15	1104.06	0.000>1
MODEL-SUMMARY	S	R^2	R^2(ADJ.)	R^2(PRED.)	
	0.708374	99.75%	99.45%	98.54%	

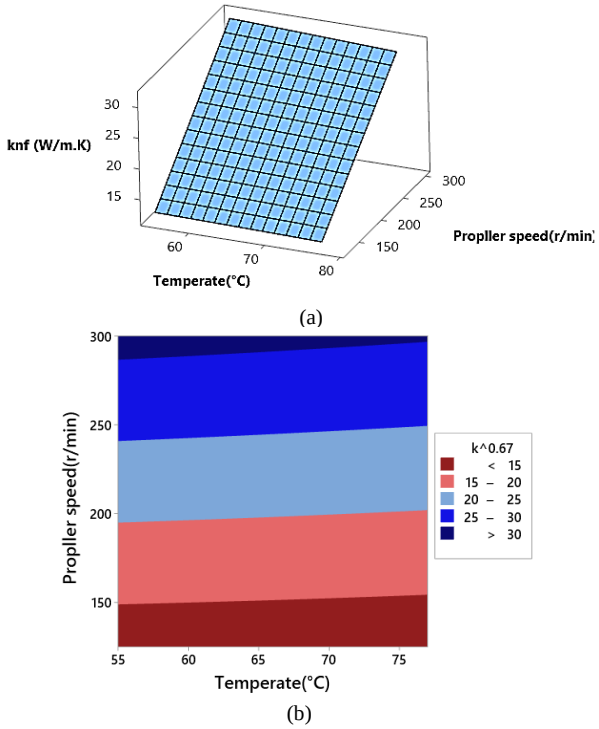

Figure 7. Shows the relationship between temperature and velocity and their effect on the thermal conductivity of nanofluids (a) Response surface plot and (b) contour plot.

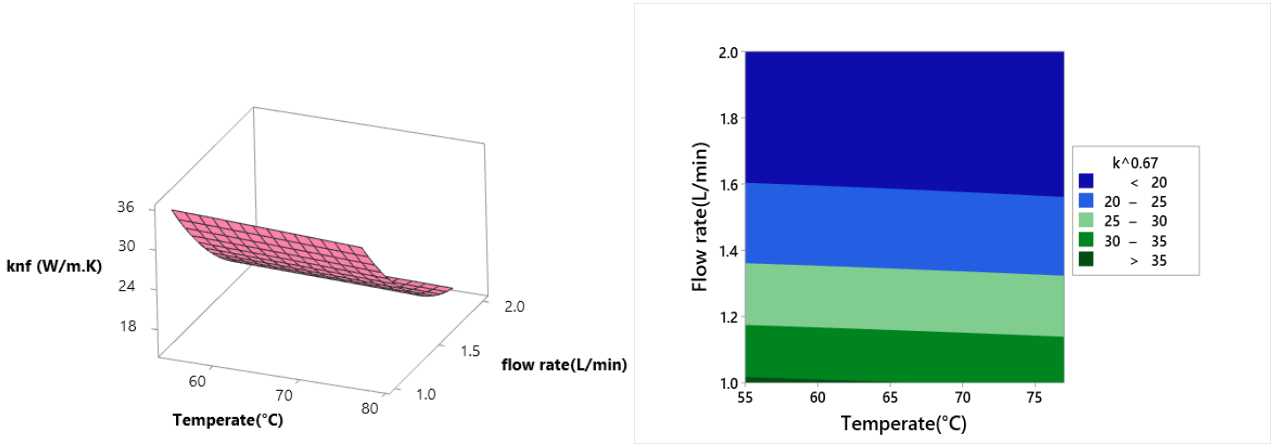

(a) (b)

Figure 8. showing the relationship between temperature and flow rate and their effect on the thermal conductivity of nanofluids (a) Response surface plot and (b) contour plot.

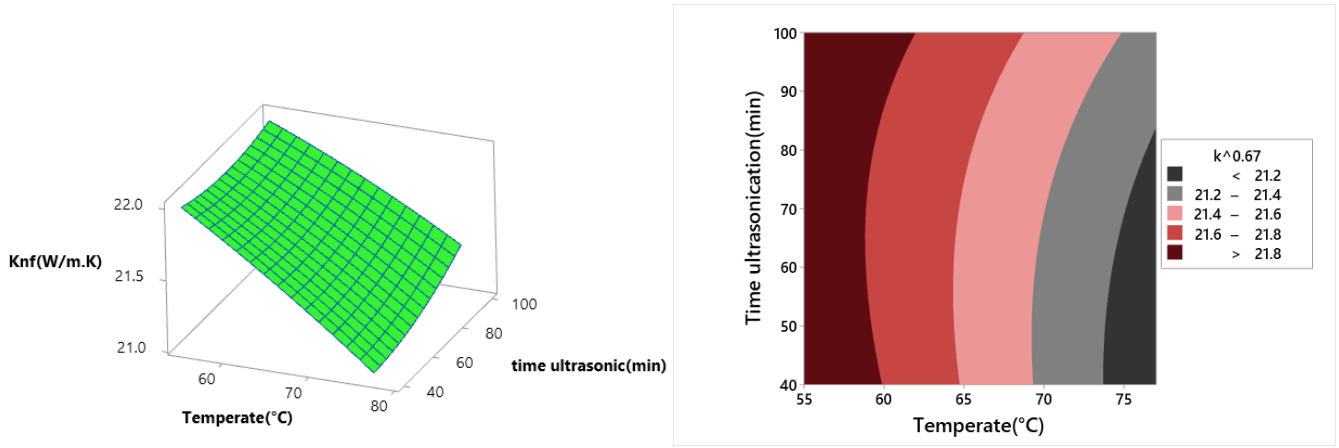

(a) (b)

Figure 9. Showing the relationship between temperature and time ultrasonic and their effect on the thermal conductivity of nanofluids (a) Response surface plot and (b) contour plot.

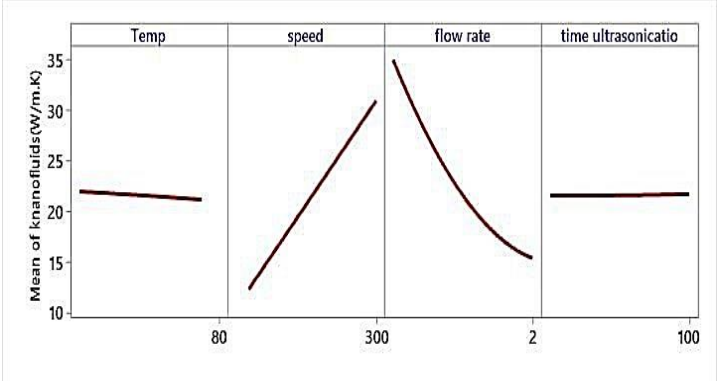

Figure 10. Shows the relationship between the speeds, temperatures, flow rates and preparation time ultrasonic on the thermal conductivity of the MWCNTs nanofluid.

Table 7. Optimum of process parameters for thermal -conductivity of nanofluids (W/m. K)

Response	Goal	Lower	Target	Upper	Weight	Importance
$K_{nanofluids}$	Maximum	9.05282	Maximum	49.3683	1	1

Solution: Parameters				Results				
Temp (°C)	Speed(r/min)	Flow rate(L/min)	Time ultrasonication (min)	Knanofluid (W/m.K) Fit	D_f	SE.Fit	95% CI	95% PI
55	300	1	100	49.3023	0.998361	1.08	(46.94, 51.66)	(46.48, 52.12)

Table 8. Confirmative value of the thermal conductivity of MWCNTs nanofluids.

Run	Temp(°C)	Speed (r/min)	Flow rate (Litter/min)	Time ultrasonication(min)	Thermal conductivity (W/m.k)		Enhancements (%)
					Actual	Average	
1	55	300	1	100	49.1	48.95	76.5752(%)
2	55	300	1	100	48.8		

Table 9. Comparing the work of previous researchers.

Researchers' names	The nanomaterial used	Process	(Enhancement% at 0.3Vol%)
[25][12]	graphite–water	Agitated Vessel	27.79%
[15][10]	Al_2O/Water	Agitated Vessel	28.9%
[23][12]	TiO_2/Water	Agitated Vessel	17.59%

The relationship shows that the longer preparation time ultrasonic leads to an increase in the thermal conductivity of the MWCNTs.
The preparation time may depend on several factors, the most important of which are particle concentration, particle size, particle type, base fluid type, etc. [26] [17] investigated the effect of ultrasound time on the heat transfer performance of MWCNT nanofluid.

7. Behavior of variables

Fig. 10 depicts the effects of temperatures and ultrasonic processing preparation time on the thermal conductivity of nanofluids, as well as their relationship, which has very little effect on thermal conductivity when compared to speeds and flow rates.

8. The optimization, confirmation test, and comparing the work of previous researchers.

Optimizing process conditions is critical and should be accomplished. Numerous standards have been identified for optimizing the system by maximizing the desired function (DF) by varying its importance or weight, which may alter the objective's characteristics. The variable's target fields have five options: maximizing, objective, minimizing, within the range, and none. The target of the thermal conductivity of MWCNT fluids was selected as "maximum," with a corresponding "weight" of 1.0. The independent parameters examined in the study have been specified in a range of designed levels: temperature from (55-77°C), speed (125–300 r/min), flow rates (1-2 L/min), and ultrasonic time (40–100 min). The lower limit value of the thermal conductivity of MWCNT nanofluids was assigned to be 9.05282 (W/m.K.), whereas the upper limit value was assigned to be 49.3683 (W/m.K.). The optimization procedure was carried out within those constraints, and the outcomes are reported in Table 7 with the function of desirability (0.998361). Two confirmatory experiments with expanded parameters were conducted to validate them; the results are shown in Table8. After 100 minutes of ultrasonic time and temperature at 55 °C, an enhancement of 76.5752% was obtained at a flow rate of 1L/min and speed of 300 r/min, which is within the range of the ideal value obtained through optimization analysis using the desirability function of 0.998361. Table 8 shows the results combining the Box-Behnken design with functional desirableness, which is effective and efficient in maximizing MWCNT and nanofluid thermal conductivity. Table 9 compares previous researchers' work and the enhancement (%) of the thermal conductivity of nanofluids obtained using different nanomaterials.

9. Conclusions

In this study, heat transfer was studied successfully in an agitated vessel reinforced with MWCNTs nanofluids using a propeller agitator. This research aims to improve heat transfer performance by using MWCNTs in distilled water to reduce energy consumption in industrial facilities in the field of heating. The experimental result shows that the response surface method is one of the most important factors affecting the thermal conductivity of MWCNTs – nanofluids. Based on the BBD, the best conditions were achieved at 55 °C, 300 rpm, 1 L/min, and an ultrasound time of 100 min, with an improved thermal conductivity of about 76.5%. Results show that RSM may be effectively used to examine various impacts and produce the necessary ideal conditions, minimizing the time, number of runs, and cost of experiments. At the same time, the Rpredict value suggests that the model is extremely suited for the experiment data. It is found that the thermal conductivity of MWCNT nanofluids in the agitated vessel depends on two main factors (speed and flow rate). Ultrasound temperature and time were found to have the least effect.

Authors' contribution
All authors contributed equally to the preparation of this article.

Declaration of competing interest
The authors declare no conflicts of interest.

Funding source
This study didn't receive any specific funds

REFERENCE

[1] B. Triveni, B. Vishwanadham, S. Venkateshwar, Studies on heat transfer to Newtonian and non-Newtonian fluids in agitated vessel, Heat and mass transfer, 44(11) (2008) 1281-1288.

[2] V. Perarasu, M. Arivazhagan, P. Sivashanmugam, Heat transfer studies in coiled agitated vessel with varying heat input, International journal of food engineering, 7(4) (2011).

[3] L. Lin, A.S. Ibrahim, X. Xu, J.M. Farber, V. Avanesian, B. Baquir, Y. Fu, S.W. French, J.E. Edwards Jr, B. Spellberg, Th1-Th17 cells mediate protective adaptive immunity against Staphylococcus aureus and Candida albicans infection in mice, PLoS pathogens, 5(12) (2009) e1000703.

[4] L. Yu, J. Ding, Injectable hydrogels as unique biomedical materials, Chemical Society Reviews, 37(8) (2008) 1473-1481.

[5] M. Chandrasekar, S. Suresh, A.C. Bose, Experimental investigations and theoretical determination of thermal conductivity and viscosity of Al2O3/water nanofluid, Experimental Thermal and Fluid Science, 34(2) (2010) 210-216.

[6] S. Suresh, K. Venkitaraj, P. Selvakumar, Comparative study on thermal performance of helical screw tape inserts in laminar flow using Al2O3/water and CuO/water nanofluids, Superlattices and Microstructures, 49(6) (2011) 608-622.

[7] Y. Rozita, R. Brydson, A. Scott, An investigation of commercial gamma-Al2O3 nanoparticles, in: Journal of Physics: Conference Series, IOP Publishing, 2010, pp. 012096.

[8] T. Arunkumar, R. Karthikeyan, R. Ram Subramani, K. Viswanathan, M. Anish, Synthesis and characterisation of multi-walled carbon nanotubes (MWCNTs), International Journal of Ambient Energy, 41(4) (2020) 452-456.

[9] B. Pak, Y. Cho, 43. BC Pak, YI Cho, Hydrodynamic and heat transfer study of dispersed fluid with subm, Exp Heat Transf, 11(2) (1998) 151-170.

[10] A. Einstein, Investigations on the Theory of the Brownian Movement, Courier Corporation, 1956.

[11] D.A. Drew, S.L. Passman, Averaged Equations, in: Theory of Multicomponent Fluids, Springer, 1999, pp. 121-130.

[12] Y. Xuan, W. Roetzel, Conceptions for heat transfer correlation of nanofluids, International Journal of heat and Mass transfer, 43(19) (2000) 3701-3707.

[13] R.H. Winterton, Where did the Dittus and Boelter equation come from?, International journal of heat and mass transfer, 41(4-5) (1998) 809-810.

[14] J. Holman, Department of Mechanical Engineering, Heat Transfer Tenth Edition Southern Methodist University, (2010).

[15] T. Perarasu, M. Arivazhagan, P. Sivashanmugam, Experimental and CFD heat transfer studies of Al2O3-water nanofluid in a coiled agitated vessel equipped with propeller, Chinese Journal of Chemical Engineering, 21(11) (2013) 1232-1243.

[16] R. Sinnott, Coulson & Richardson's chemical engineering, vol. 6, Chemical engineering design, 4 (2005).

[17] M. Soltanimehr, M. Afrand, Thermal conductivity enhancement of COOH-functionalized MWCNTs/ethylene glycol–water nanofluid for application in heating and cooling systems, Applied Thermal Engineering, 105 (2016) 716-723.

[18] M.A. Bezerra, R.E. Santelli, E.P. Oliveira, L.S. Villar, L.A. Escaleira, Response surface methodology (RSM) as a tool for optimization in analytical chemistry, Talanta, 76(5) (2008) 965-977.

[19] J. Segurola, N.S. Allen, M. Edge, A. Mc Mahon, Design of eutectic photoinitiator blends for UV/visible curable acrylated printing inks and coatings, Progress in Organic Coatings, 37(1-2) (1999) 23-37.

[20] Q. Zhao, J.F. Kennedy, X. Wang, X. Yuan, B. Zhao, Y. Peng, Y. Huang, Optimization of ultrasonic circulating extraction of polysaccharides from Asparagus officinalis using response surface methodology, International journal of biological macromolecules, 49(2) (2011) 181-187.

[21] R. Arunachalam, G. Annadurai, Optimized response surface methodology for adsorption of dyestuff from aqueous solution, Journal of environmental science and technology, 4(1) (2011) 65-72.

[22] X.-Q. Wang, A.S. Mujumdar, Heat transfer characteristics of nanofluids: a review, International journal of thermal sciences, 46(1) (2007) 1-19.

[23] V. Perarasu, M. Arivazhagan, P. Sivashanmugam, Heat transfer of TiO2/water nanofluid in a coiled agitated vessel with propeller, Journal of Hydrodynamics, 24(6) (2012) 942-950.

[24] A. Gulhane, S. Chincholkar, Experimental investigation of convective heat transfer coefficient of Al2O3/water nanofluid at lower concentrations in a car radiator, Heat Transfer—Asian Research, 46(8) (2017) 1119-1129.

[25] P. Sivashanmugam, H. Mothilal, Experimental heat transfer behavior of graphite–water microfluid in a coiled agitated vessel, Heat Transfer—Asian Research, 47(3) (2018) 492-506.

[26] V. Sridhara, B. Gowrishankar, Snehalatha, L. Satapathy, Nanofluids—a new promising fluid for cooling, Transactions of the Indian Ceramic Society, 68(1) (2009) 1-17.